

Phase transition and properties of compact star

B.K. Sharma, P.K. Panda, and S.K. Patra

Institute of Physics, Sachivalaya Marg, Bhubaneswar - 751 005, India.

We investigate the phase transition to a deconfined phase and the consequences in the formation of neutron stars. We use the recently proposed effective field theory motivated relativistic mean field theory for hadron and the MIT Bag model and color-flavor locked (CFL) phase for the quark matter in order to get the appropriate equation of state. The properties of star are then calculated. The differences between unpaired and CFL quark matter are discussed.

PACS numbers:

I. INTRODUCTION

One of the fundamental problem of nuclear physics is to understand the behavior of nuclear matter at extreme conditions. The study of neutron star provide an important information in this regard. Neutron star are extremely dense objects. They formed after the gravitational core collapse of a massive star [1]. The environment in central region resembles the early universe, except that the temperature (T) is lower. Due to the lower temperature and high density, neutron stars are presumably unique astrophysical laboratories for a broad range of physical phenomena [1, 2]. The composition and other properties of neutron stars are depend upon the appropriate equation of state (EOS) that describe its crust and interior region [3]. The crust part of neutron star, where the density is comparable to saturation density (ρ_0) of symmetric nuclear matter, is adequately described by hadronic matter. But the interior region where density ρ is of the order of 5 to 10 times of ρ_0 , a phase transition occurs from hadronic to quark matter. But this is not well understood, whether the interface region, it is a quark and/or mixed matter. It is reasonable to assume that the central part is dense enough, so that it can be treated as a pure quark phase. However, the boundary part between the quark and hadronic matter should be an admixture of quark and baryonic degrees of freedom. In the present study, we are interested in building the EOS for mixed matter of quark and hadron phases. We employ an effective field theory motivated (E-RMF) Lagrangian approach including hyperons in order to describe the hadron phase. For the quark phase we have chosen to use both unpaired quark matter (UQM) described by the MIT bag model [4, 5, 6, 7] and paired quarks described by the color-flavor locked (CFL) phase. Recently many authors [8, 9, 10, 11, 12, 13, 14] have discussed the possibility that the quark matter is in a color superconducting phase, in which quarks near the Fermi surface are paired, forming Cooper pairs which condense and break the color gauge symmetry [15]. At sufficiently high density the favored phase is called CFL, in which quarks of all three colors and all three flavors are allowed to pair.

phase for quark matter and mixed phase are described. Here, we are trying to build an equation of state for mixed matter of hadron and quark phases. We use an E-RMF model including hyperons with incompressibility $K = 300$ MeV and $M^*/M = 0.7$ of nuclear matter for hadron phase. We use Gibbs criteria and chemical equilibrium conditions, to built a mixed phase EOS, and then we calculate and discuss the properties of star at T=0. The calculated results are discussed in section III. In the last section, the conclusions are drawn.

II. FORMALISM

A. Hadron matter

In principle, one should use quantum chromodynamics (QCD), the fundamental theory of strong interaction, for the complete description of EOS. But it cannot be use to describe hadronic matter due to its non-perturbative properties. A major breakthrough occurred when the concept of effective field theory (EFT) was introduced and applied to low energy QCD [16]. The EFT for strong interaction at low energy is known as quantum hadrodynamics (QHD) [17, 18, 19, 20, 21]. The mean field treatment of QHD has been used extensively in order to describe properties of nuclear matter [17, 22] and finite nuclei [23, 24, 25, 26]. The degrees of freedom in this theory are nucleons interacting through the exchange of iso-scalar scalar σ , iso-scalar vector ω , iso-vector-vector ρ and the pseudoscalar π mesons. The nucleons are considered as Dirac particle moving in classical meson fields. The contribution of π meson is zero at mean field level, due to pseudo-spin nature. The chiral effective Lagrangian (E-RMF) proposed by Furnstahl, Serot and Tang [27, 28, 29] is the extension of the standard relativistic mean field (RMF) theory with the addition of non-linear scalar-vector and vector-vector self interaction. This Lagrangian includes all the non-renormalizable couplings consistent with the underlying symmetries of QCD. Applying the naive dimensional analysis [30, 31] and the concept of naturalness one can expand the nonlinear Lagrangian and organize it in increasing powers of the fields and their derivatives and

tice, to get a reasonable result, one needs the Lagrangian up to 4th order of interaction. In the interior of neutron star, where the density is very high, other hadronic states are produced [1, 35, 36, 37]. Thus, the consid-

ered model involves the full octet of baryons interacting through mesons. The truncated Lagrangian which includes the terms up to the fourth order is given by

$$\begin{aligned} \mathcal{L} = & \bar{\Psi}_B (i\gamma^\mu D_\mu - m_B + g_{\sigma B}\sigma) \Psi_B + \frac{1}{2}\partial_\mu\sigma\partial^\mu\sigma - m_\sigma^2\sigma^2 \left(\frac{1}{2} + \frac{\kappa_3}{3!}\frac{g_{\sigma B}\sigma}{m_B} + \frac{\kappa_4}{4!}\frac{g_{\sigma B}^2\sigma^2}{m_B^2} \right) - \frac{1}{4}\Omega_{\mu\nu}\Omega^{\mu\nu} \\ & + \frac{1}{2}\left(1 + \eta_1\frac{g_{\sigma B}\sigma}{m_B} + \frac{\eta_2}{2}\frac{g_{\sigma B}^2\sigma^2}{m_B^2}\right)m_\omega^2\omega_\mu\omega^\mu - \frac{1}{4}R_{\mu\nu}^\alpha R^{\alpha\mu\nu} + \left(1 + \eta_\rho\frac{g_{\sigma B}\sigma}{m_B}\right)\frac{1}{2}m_\rho^2\rho_\mu^\alpha\rho^{\alpha\mu} + \frac{1}{4!}\zeta_0 g_{\omega B}^2 (\omega_\mu\omega^\mu)^2 \end{aligned} \quad (1)$$

The subscript $B = n, p, \Lambda, \Sigma$ and Ξ , denotes for baryons. The terms in eqn. (1) with the subscript "B" should be interpreted as sum over the states of all baryonic octets. The covariant derivative D_μ is defined as

$$D_\mu = \partial_\mu + ig_{\omega B}\omega_\mu + ig_{\phi B}\phi_\mu + ig_{\rho B}I_{3B}\tau^a\rho_\mu^a, \quad (2)$$

whereas $R_{\mu\nu}^\alpha$, and $\Omega_{\mu\nu}$ are the field tensors

$$R_{\mu\nu}^\alpha = \partial_\mu\rho_\nu^\alpha - \partial_\nu\rho_\mu^\alpha + g_\rho\epsilon_{abc}\rho_\mu^b\rho_\nu^c, \quad (3)$$

$$\Omega_{\mu\nu} = \partial_\mu\omega_\nu - \partial_\nu\omega_\mu, \quad (4)$$

where m_B denotes the baryon and $m_\sigma, m_\omega, m_\rho$ are the masses assigned to the meson fields. Using this Lagrangian, we derive the equation of motion and solved it in the mean field approximation self consistently. Here, the meson fields are replaced by their classical expectation values. The field equations for σ, ω and ρ -meson are given by

$$m_\sigma^2\left(\sigma_0 + \frac{g_{\sigma B}\kappa_3}{2m_B}\sigma_0^2 + \frac{g_{\sigma B}^2\kappa_4}{6m_B^2}\sigma_0^3\right) - \frac{1}{2}m_\omega^2\left(\eta_1\frac{g_{\sigma B}}{m_B} + \eta_2\frac{g_{\sigma B}^2}{m_B^2}\sigma_0\right)\omega^2 - \frac{1}{2}m_\rho^2\eta_\rho\frac{g_\sigma}{m_B}\rho_0^2 = \sum_B g_{\sigma B}m_B^{*2}\rho_{SB} \quad (5)$$

$$m_\omega^2\left(1 + \frac{\eta_1 g_\sigma}{m_B}\sigma_0 + \frac{\eta_2 g_\sigma^2}{2m_B^2}\sigma_0^2\right)\omega_0 + \frac{1}{6}\zeta_0 g_{\omega B}^2\omega_0^3 = \sum_B g_{\omega B}\rho_B \quad (6)$$

$$m_\rho^2\left(1 + \frac{g_{\sigma B}\eta_\rho}{m_B}\sigma_0\right)\rho_{03} = \sum_B g_{\rho B}I_{3B}\rho_B \quad (7)$$

For a baryon species, the scalar density, ρ_{SB} , and baryon density (ρ_B) are

$$\rho_{SB} = \frac{2J_B + 1}{2\pi^2} \int_0^{k_B} \frac{k^2 dk}{E_B^*} \quad (8)$$

$$\rho_B = \frac{2J_B + 1}{2\pi^2} \int_0^{k_B} k^2 dk \quad (9)$$

where $E_B^* = \sqrt{k^2 + m_B^{*2}}$ is the effective energy and J_B and I_{3B} are the spin and isospin projection of baryon B , the quantity k_B is the Fermi momentum for the baryon, $m^* = m_B - g_{\sigma B}\sigma$ is the effective mass, which is solve self-consistently from equation (5). After obtaining the self-consistent fields, the pressure P and total energy density ε for a given baryon density are

$$\begin{aligned} P = & \frac{\gamma}{3(2\pi)^3} \int_0^{k_B} d^3k \frac{k^2}{E_B^*(k)} + \frac{1}{4!}\zeta_0 g_{\omega B}^2\omega_0^4 + \frac{1}{2}\left(1 + \eta_1\frac{g_{\sigma B}\sigma_0}{m_B} + \frac{\eta_2}{2}\frac{g_{\sigma B}^2\sigma_0^2}{m_B^2}\right)m_\omega^2\omega_0^2 \\ & - m_\sigma^2\sigma_0^2\left(\frac{1}{2} + \frac{\kappa_3 g_{\sigma B}\sigma_0}{3!m_B} + \frac{\kappa_4 g_{\sigma B}^2\sigma_0^2}{4!m_B^2}\right) + \frac{1}{2}\left(1 + \eta_\rho\frac{g_{\sigma B}\sigma_0}{m_B}\right)m_\rho^2\rho_0^2 + \sum P_l, \end{aligned} \quad (10)$$

$$\begin{aligned} \varepsilon = & \frac{\gamma}{(2\pi)^3} \int_0^{k_B} d^3k E_B^*(k) + \frac{1}{8} \zeta_0 g_{\omega B}^2 \omega_0^4 + \frac{1}{2} \left(1 + \eta_1 \frac{g_{\sigma B} \sigma_0}{m_B} + \frac{\eta_2 g_{\sigma B}^2 \sigma_0^2}{2 m_B^2} \right) m_{\omega B}^2 \omega_0^2 \\ & + m_{\sigma B}^2 \sigma_0^2 \left(\frac{1}{2} + \frac{\kappa_3 g_{\sigma B} \sigma_0}{3! m_B} + \frac{\kappa_4 g_{\sigma B}^2 \sigma_0^2}{4! m_B^2} \right) + \frac{1}{2} \left(1 + \eta_\rho \frac{g_{\sigma B} \sigma_0}{m_B} \right) m_\rho^2 \rho_0^2 + \sum_l \varepsilon_l, \end{aligned} \quad (11)$$

As explained earlier, the terms in equations (10) and (11) with the subscript "B" should be interpreted as sum over the states of all baryonic octets and $\gamma = 2$ is the spin degeneracy. In the above, P_l and ε_l are lepton pressure and energy density respectively, explained in the following subsections.

For stars in which the strongly interacting particles are baryons, the composition is determined by the requirements of charge neutrality and β -equilibrium conditions under the weak processes $B_1 \rightarrow B_2 + l + \bar{\nu}_l$ and $B_2 + l \rightarrow B_1 + \nu_l$. After deleptonization, the charge neutrality condition yields

$$q_{\text{tot}} = \sum_B q_B (2J_B + 1) k_B^3 / (6\pi^2) + \sum_{l=e,\mu} q_l k_l^3 / (3\pi^2) = 0, \quad (12)$$

where q_B corresponds to the electric charge of baryon species B and q_l corresponds to the electric charge of lepton species l . Since the time scale of a star is effectively infinite compared to the weak interaction time scale, weak interaction violates strangeness conservation. The strangeness quantum number is therefore not conserved in a star and the net strangeness is determined by the condition of β -equilibrium which for baryon B is then given by $\mu_B = b_B \mu_n - q_B \mu_e$, where μ_B is the chemical potential of baryon B and b_B its baryon number. Thus the chemical potential of any baryon can be obtained from the two independent chemical potentials μ_n and μ_e of neutron and electron respectively.

The lepton Fermi momenta are the positive real solutions of $(k_e^2 + m_e^2)^{1/2} = \mu_e$ and $(k_\mu^2 + m_\mu^2)^{1/2} = \mu_\mu = \mu_e$. The equilibrium composition of the star is obtained by solving the set of Eqs. (5)- (7) in conjunction with the charge neutrality condition (12) at a given total baryonic density $\rho = \sum_B (2J_B + 1) k_B^3 / (6\pi^2)$; the baryon effective masses are obtained self-consistently.

B. Unpaired Quark Matter

In the central part of neutron star the density is expected to high enough that hadronic matter undergoes to quark degrees of freedom. In quark phase we employ MIT bag model to describe unpaired quark matter [38, 39, 40]. The bag model provides a useful phenomenological description of quarks being confined inside the hadrons. Confinement results from the balance of the bag pressure on the bag walls from the outside and the pressure resulting from the kinetic energy of the quarks inside the

which the u,d and s quark are degrees of freedom with electron. In this model the masses of u and d are set to 5.0 MeV and strange quark mass is taken to be 150 MeV. The chemical equilibrium is given by

$$\mu_d = \mu_s = \mu_u + \mu_e \quad (13)$$

The μ_n and μ_e are the two independent chemical potentials and rest can be written in terms of them as follows:

$$\mu_u = \frac{1}{3} \mu_n - \frac{2}{3} \mu_e \quad (14)$$

$$\mu_d = \frac{1}{3} \mu_n + \frac{1}{3} \mu_e \quad (15)$$

$$\mu_s = \frac{1}{3} \mu_n + \frac{1}{3} \mu_e \quad (16)$$

The pressure for quark flavor f , with $f = u, d$ or s is [41]

$$P_q = \frac{1}{4\pi^2} \sum_f [\mu_f k_f (\mu_f^2 - \frac{5}{2} m_f^2) + \frac{3}{2} m_f^4 \ln \frac{\mu_f + k_f}{m_f}] \quad (17)$$

where $k_f = (\mu_f^2 - m_f^2)^{1/2}$ is the fermi momentum.

The leptons pressure is

$$P_l = \frac{1}{3\pi^2} \sum_l \int \frac{p^4 dp}{(p^2 + m_l^2)^{1/2}} \quad (18)$$

The total pressure is given by

$$P = P_l + P_q - B \quad (19)$$

where B is the bag constant.

C. Color Flavor Locked Quark Matter

In this section, we consider the quark matter phase as color flavor locked (CFL) quark paired, in which the quark near the Fermi surface form Cooper pairs which condense, breaking the color gauge symmetry. In CFL phase, all the three colors and three flavors are allowed to pair and this is the favored phase at sufficiently high density. We describe the CFL phase by using the ther-

$$\Omega_{CFL}(\mu_q, \mu_e) = \Omega_{quarks}(\mu_q) + \Omega_{GB}(\mu_q, \mu_e) + \Omega_l(\mu_e), \quad (20)$$

where $\mu_q = \frac{\mu_n}{3}$ and

$$\Omega_{quarks}(\mu_q) = \frac{3}{\pi^2} \sum_{f=u,d,s} \int_0^\nu p^2 dp \left(\sqrt{p^2 + m_f^2} - \mu_q \right) - \frac{3\Delta^2 \mu_q^2}{\pi^2} + B \quad (21)$$

$$\nu = \sqrt{\mu_q^2 + \frac{m_u^2}{3}} + \sqrt{\mu_q^2 + \frac{m_d^2}{3}} - \sqrt{\mu_q^2 + \frac{m_s^2}{3}} \quad (22)$$

and the Goldstone boson contribution due to chiral symmetry breaking in the CFL phase is given by

$$\Omega_{GB}(\mu_q, \mu_e) = -\frac{1}{2} f_\pi^2 \mu_e^2 \left(1 - \frac{m_\pi^2}{\mu_e^2} \right)^2 \quad (23)$$

where the parameters are

$$f_\pi^2 = \frac{(21 - 8 \ln 2) \mu^2}{36\pi^2}, \quad (24)$$

$$m_\pi^2 = \frac{3\Delta^2}{\pi^2 f_\pi^2} m_s (m_u + m_d) \quad (25)$$

and the electron contribution Ω_l is given by

$$\Omega_l(\mu_e) = -\frac{\mu_e^4}{12\pi^2} \quad (26)$$

The quark number densities and the electrical charge density carried by the pion is given by

$$\rho_u = \rho_d = \rho_s = \frac{\nu^3 + 2\Delta^2 \mu_q}{\pi^2} \quad (27)$$

where Δ is gap parameter and its value is 100 MeV, which is the typical value considered in the literature.

The electric charge density carried by the pion condensate is given by

$$\rho_{CFL} = -f_\pi^2 \mu_e \left(1 - \frac{m_\pi^4}{\mu_e^4} \right). \quad (28)$$

In the above thermodynamic potential, we have neglected the contribution due to the kaon condensation which is an effect of order m_s^4 and thereby small compared to the $\Delta^2 \mu_q^2$ contribution to the thermodynamic potential for $\Delta \sim 100$ MeV.

D. Mixed Phase and Star Properties

The mixed phase is obtained by applying charge neutrality condition and Gibbs criteria for hadron and quark phase. The charge neutrality condition is:

$$\rho_c^{QP} + (1 - \chi) \rho_c^{HP} + \rho_e = 0 \quad (29)$$

where ρ_c^{QP} and ρ_c^{HP} are the charge density of quark and hadron phase, χ and $(1 - \chi)$ are the volume fraction occupied by quark and hadron phase respectively. The phase boundary of the coexistence region between the hadron phase and quark phase is determined by Gibbs criteria. The critical pressure, critical neutron and electron chemical potentials are determined by the conditions:

$$\mu_{HP,i} = \mu_{QP,i} = \mu_i, \quad i = n, e \quad (30)$$

$$T_{HP} = T_{QP}, \quad (31)$$

$$P_{HP}(\mu_{HP}, T) = P_{QP}(\mu_{QP}, T), \quad (32)$$

These are the chemical, thermal and mechanical equilibrium, respectively. The energy and the total baryon densities in the mixed phase are:

$$\varepsilon = \chi \varepsilon^{QP} + (1 - \chi) \varepsilon^{HP} + \varepsilon^l, \quad (33)$$

and

$$\rho = \chi \rho^{QP} + (1 - \chi) \rho^{HP}. \quad (34)$$

Once the above quantities are obtained, we can construct the EOS for mixed phase and consequently compute the properties of neutron star. To evaluate the star structure we use the Tolman-Oppenheimer-Volkoff (TOV) equations found in Ref. [42]. They are

$$\frac{dP}{dr} = -\frac{G}{r} \frac{[\varepsilon + P][M + 4\pi r^3 P]}{r - 2GM}, \quad (35)$$

$$\frac{dM}{dr} = 4\pi r^2 \varepsilon \quad (36)$$

where G and $M(r)$ are the gravitational constant and enclosed gravitational mass and $c = 1$. For a given EOS, these equations can be integrated from the origin as an initial value problem for a given choice of the central density, (ε_0) . The value of $r(= R)$ at which the pressure

III. RESULTS AND DISCUSSIONS

We obtain the EOS for hadronic matter by changing incompressibility $K=300$ MeV and effective mass (M^*/M) to 0.7 of G2 parameter set [43]. It is to be noted that we are not getting any mixed phase with original G2 set. So we change the incompressibility K from 215 MeV to 300

MeV and effective mass (M^*/M) from 0.664 to 0.7. The resultant parameter set satisfies all the nuclear saturation properties so that our extrapolation to higher density remains meaningful. After the above re-adjustment, the modified Lagrangian parameters are given in Table I. To compare the changes, the original G2 set is also displayed in the Table.

TABLE I: G2 and modified G2 parameter set (G2*)

Set	m_s/M	m_ω/M	m_ρ/M	$g_s/4\pi$	$g_\omega/4\pi$	$g_\rho/4\pi$	κ_3	κ_4	ζ_0	η_1	η_2	η_ρ
G2*	0.554	0.833	0.820	0.751	0.936	0.614	1.202	14.981	2.642	0.650	0.110	0.390
G2	0.554	0.833	0.820	0.835	1.016	0.755	3.247	0.632	2.642	0.650	0.110	0.390

We assume that all the hyperons in the octet have the same couplings. They are expressed as a ratio to the nucleon coupling $x_\sigma = x_{H\sigma}/x_{N\sigma} = \sqrt{\frac{2}{3}}$, $x_\omega = x_{H\omega}/x_{N\omega} = \sqrt{\frac{2}{3}}$ and $x_\rho = x_{H\rho}/x_{N\rho} = \sqrt{\frac{2}{3}}$. Using the modified values of G2 set of Table I, the EOS for quark matter obtained with unpaired quark model and color flavor locked phase for different values of the Bag pressure B . In our calculation, we took $B^{\frac{1}{4}} = 170$ MeV, 188 MeV for UQM and CFL models respectively, and then calculate the equation of state. For the CFL, it is to be noted that we do not find any mixed phase at $B^{\frac{1}{4}} = 170$ MeV and 180 MeV. In both the cases we have $m_u = m_d = 5$ MeV and $m_s = 150$ MeV.

In Fig. 1 we plot the resulting EOS for both E-RMF+UQM and E-RMF+CFL cases. From Fig. 1 it is evident that the mixed phase starts earlier in case of UQM whereas CFL predicts the mixed phase at higher density approximately at around $\varepsilon = 2 \text{ fm}^{-4}$. The inclusion of hyperons softens the EOS [44] of the charge neutral dense matter. This is clearly seen from the change in the slope of Fig. 1 for energy density greater than $\varepsilon \approx 2.2 \text{ fm}^{-4}$.

In Fig.2, the fractional particle densities, ρ_i/ρ_0 for baryons, leptons and quarks in E-RMF+UQM are shown. From the Fig.2, we notice the onset of quarks at around $1.3\rho_0$ and immediately in the vicinity of $4\rho_0$ they are the most abundant particle in the matter. With increasing density the model predicts pure quark matter after $6\rho_0$. At this density and thereafter all the three quarks under consideration contributes almost equally to the matter density. As evident from the figure that the leptonic contribution ceases after $4\rho_0$, which are primarily used up to maintain charge neutrality of the matter. The nucleons constitutes a sizeable population in the matter but after they decrease abruptly at around $5\rho_0$, after which it is a pure quark phase. Further it can be seen that Λ

particle fraction decreases, finally ends at around $6\rho_0$. The appearance of Λ is decided purely by the neutron chemical potential since it is isospin independent and hence the density of Λ decreases with decrease in neutron density. However the contribution of Λ is quite negligible overall.

In Fig.3, the particle population for the baryons, leptons and quarks are shown as a function of baryon density up to $8\rho_0$ in case of E-RMF+CFL for $B^{\frac{1}{4}} = 188 \text{ MeV}$. From the Fig., it can be seen that the appearance of quark starts $\sim 2.5\rho_0$. It is to be noted that the quarks are of equal densities in CFL. The deleptonization in the matter occurs at $\sim 5.5\rho_0$. Similarly, the nucleons follows similar trend and at $\sim 5.5\rho_0$ the matter is in pure quark phase. Like Fig.2, Λ appears at $4\rho_0$ and decrease with the nucleons particle fractions and finally ends at $5.5\rho_0$. In CFL case, Σ^- appears at $1.89 \rho_0$ and ends at $3.5\rho_0$. In both the cases i.e., E-RMF+UQM and E-RMF+CFL the difference is due to the different charge neutrality conditions.

The strangeness content in case of high density matter is an exciting possibility, which can give important insights into some of the most fundamental problems of astrophysics and high density behavior. Figure 4 displays the strangeness content in the core and the crust of the neutron star as obtained in our calculations. The strangeness content is given by

$$r_s = \chi r_s^{QP} + (1 - \chi) r_s^{HP}. \quad (37)$$

with

$$r_s^{QP} = \frac{\rho_s}{3\rho}, r_s^{HP} = \frac{\sum_B |q_s^B| \rho_B}{3\rho} \quad (38)$$

where q_s^B is the strange charge of baryon B . In both the cases, the strangeness fraction rises steadily. However in case of UQM the onset of strangeness starts at around $1.3 \rho_0$ and gets saturated at around $6.0 \rho_0$ where the matter

content in CFL starts at around 2 times normal nuclear matter density, then rises steadily in the mixed phase and ultimately gets saturated at $\sim 6.6\rho_0$. Using the EOS corresponding to the UQM and CFL we now compute the properties of hybrid neutron star similar to the case of pure neutron star mass, M_\odot and radius, gravitational red shift (Z), the baryonic mass of the star, M_b .

In Fig. 5 the maximum mass of the hybrid star is plotted as a function of the radius of the star as obtained by the UQM and CFL model in our calculations. The radius of the maximum mass of the star is sensitive to the low density EOS. In order to calculate the radius and to plot it versus the star mass, we have used the results of Baym, Pethick and Sutherland [45] for low baryonic densities. The maximum mass obtained are $1.44 M_\odot$ and $1.35 M_\odot$ for UQM and CFL respectively. The corresponding radius obtained are 9.35 km and 9.33 km respectively. These results are found to be in good agreement with different field theoretical models and also from observational point of view [46, 47]. The success of the model is evident from figure 7, where we plot M/R ratios as reported by [46, 47].

Constraints on the mass-to-radius ratio can be obtained from accurate measurements of the gravitational red shift of spectral lines produced in neutron star photospheres. As already mentioned that a red shift of 0.35 from three different transitions of the spectra of the X-ray binary EXO0748-676 was obtained [46], which corresponds to $M/R = 0.15 M_\odot/km$. Another constraint to the mass-to-radius ratio given by $M/R = 0.069 M_\odot/km$ to $M/R = 0.115 M_\odot/km$ was determined from the observation of two absorption features in the source spectrum of the 1E 1207.4-5209 neutron star [47]. However, in the second case, the interpretation of the absorption features as atomic transition lines is controversial. The absorption features are of cyclotron nature which make the related constraints unrealistic [48, 49]. In our calculations the M/R ratio comes out to be 0.15 and 0.14 for UQM and CFL respectively. It is evident that our results are in very good agreement with the observed analysis. We have added the lines corresponding to those constraints shown by straight lines in Fig.5.

Baryonic mass as a function of maximum mass of the star is plotted in Fig. 6. It is to be noted that the baryonic mass always exceeds the maximum mass, which is typical of the compact objects. The difference between the two is defined as the gravitational binding of the star. The baryonic mass, $M_b(M_\odot)$, obtained by UQM and CFL are $1.63 M_\odot$ and $1.51 M_\odot$ respectively.

Gravitational red shift of a star is an important property that is defined as

$$Z = \frac{1}{\sqrt{1 - 2GM/Rc^2}}. \quad (39)$$

Red shift primarily depends on the M/R ratio of the star and observationally in absence of precise and direct measurements of mass and radius of the star it serves the

TABLE II: Calculated properties of Neutron star

EOS	$M(M_\odot)$	$E_c (10^{14} gcm^{-3})$	$R(km)$	$M_b(M_\odot)$	Z
UQM	1.44	31.0	9.35	1.62	0.35
CFL	1.35	32.0	9.33	1.51	0.32

7, we plot the gravitational red shift as a function of mass of the star with the straight lines as observational constraints. The two solid straight lines are corresponds to red shift $Z = 0.12 - 0.23$ was determined from the observation of two absorption features in the source spectrum of the 1E 1207.4-5209 neutron star [47] and the dotted dash line is correspond to $Z = 0.35$ which is determined from three different transitions of the spectra of the X-ray binary EXO0748-676 [46]. In our calculation, we obtained $Z = 0.35$ and $Z = 0.32$ for UQM and CFL respectively. Our results are in good agreement with the data. For the sake of completeness, we present the overall results in Table II.

IV. SUMMARY AND CONCLUSIONS

In the summary, we obtained the EOS of state for neutron star and studied the various properties of the star i.e., like mass, radius and redshift. The phase transitions from hadron to quark matter and the existence of the mixed phase in the inner core of the star are analyzed. The considered model based on the assumption that the neutron star consists of the inner core and crusts as two main parts of it. The theoretical model [27] for the outer region is described by the Lagrangian which includes the full octet of baryons interacting through the exchange of meson fields. The chosen parameter set based on effective field theory motivated relativistic mean field includes nonlinear scalar-vector and vector-vector interaction terms which leads to the soft EOS. This is in agreement of DBHF results. But the mixed phase EOS are not feasible, within the original G2 parameter set of the E-RMF formalism. To get a reasonable EOS for the mixed phase, for the hadronic matter, we changed the incompressibility marginally.

The inner core of the star is described by UQM and CFL models. In UQM the quarks are treated as massless particles inside a bag of finite dimension and confinements results from the balance of the pressure on the bag walls from the outside and the bag pressure resulting from the kinetic energy of the quarks inside the bag. The CFL phase consists of equal numbers of u,d and s quark and so requires no electrons to make it electrically neutral. In this paper we used different bag pressure $B_{\frac{1}{4}} = 170$ MeV and 188 MeV for UQM and CFL model, respectively.

The EOS are then employed to study and evaluate the global properties of the hybrid neutron star like mass, radius and gravitational redshift Z . The masses are predicted to be 1.44 and 1.35 for UQM and CFL model respectively. The radii are 9.35 and 9.33 km for UQM and CFL model respectively. The gravitational red shift is 0.35 and 0.32 for UQM and CFL model respectively.

9.33 km in E-RMF+UQM and E-RMF+CFL models, respectively. We have also shown that the EOS with UQM and CFL quark phase satisfies the constraint imposed by the recently measured redshift of 0.35 from three different transitions of the spectra of the X-ray binary EXO0748-676 [46]. The redshifts are 0.35 and 0.32 in the E-RMF+UQM and E-RMF+CFL formalism, respectively, which coincides very well with the measurement.

ACKNOWLEDGMENTS

One of the authors (PKP) is thankful to Institute of Physics for support of this research work. This work was partially supported by CSIR, Govt. of India under the project No. 03(1060)/06/EMR-II.

-
- [1] N. K. Glendenning, *Compact Stars, Nuclear Physics, Particle Physics and General Relativity* (Springer-Verlag, New York, 1997).
- [2] S. L. Shapiro and S. A. Teukolsky, *Black Holes, White Dwarfs, and Neutron Stars* (John Wiley, New York, 1983).
- [3] P. Danielwicz, R. Lacey, W. G. Lynch, *Science* **298**, 1592 (2002).
- [4] A. Chodos, R.L. Jaffe, K. Johnson, C.B. Thorne and V.F. Weisskopf, *Phys. Rev. D* **9**, (1974) 3471.
- [5] B. Freedman and L. McLerran, *Phys. Rev. D* **17**, 1109 (1978).
- [6] E. Farhi and R.L. Jaffe, *Phys. Rev. D* **30**, 2379 (1984).
- [7] J.I. Kapusta, *Finite Temperature Field Theory* (Cambridge University Press)
- [8] I. Shovkovy, M. Hanauske, M. Huang, *Phys. Rev. D* **67**, 103004 (2003).
- [9] M. Alford and S. Reddy, *Phys. Rev. D* **67**, 074024 (2003).
- [10] M. Buballa and M. Oertel, *Nucl. Phys. A* **703**, 770 (2002); M. Baldo, M. Buballa, G.F. Burgio, F. Neumann, M. Oertel and H.-J. Schulze *Phys. Lett B* **562**, 153 (2003).
- [11] A.W. Steiner, S. Reddy and M. Prakash, *Phys. Rev. C* **66**, 094007 (2002).
- [12] M. Alford, K. Rajagopal, S. Reddy, F. Wilczek, *Phys. Rev. D* **64**, 074017 (2001).
- [13] K. Rajagopal, and F. Wilczek, *Phys. Rev. Lett.* **86**, 3492 (2001).
- [14] P. K. Panda, D.P. Menezes, C. Providencia, *Phys. Rev. C* **69** 025207 (2004); P. K. Panda, D.P. Menezes, C. Providencia, *Phys. Rev. C* **69** 058801 (2004); P. K. Panda, H.S. Nataraj, *Phys. Rev. C* **73** 025807 (2006).
- [15] M.G. Alford, *Annu. Rev. Nucl. Part. Sci.* **51**, 131 (2001).
- [16] S. Weinberg *Physica* **96A**, 327 (1979).
- [17] J. D. Walecka, *Ann. Phys. (N.Y.)* **83**, 491 (1974).
- [18] B. D. Serot and J. D. Walecka, *Adv. Nucl. Phys.* **16**, 1 (1986).
- [19] P. -G. Reinhard, *Rep. Prog. Phys.* **52**, 439 (1989).
- [20] B. D. Serot, *Rep. Prog. Phys.* **55**, 1855 (1992).
- [21] B. D. Serot and J. D. Walecka, *Int. J. Mod. Phys. E* **6**, 515 (1997).
- [22] P. Arumugam, B. K. Sharma, P. K. Sahu, S. K. Patra Tapas Sil, M. Centelles and X. Viñas, *Phys. Lett.* **B601**, 51 (2004).
- [23] C.J. Horowitz and B.D. Serot, *Nucl. Phys.* **A368**, 503 (1981).
- [24] J. Boguta and A. R. Bodmer, *Nucl. Phys.* **A292**, 413 (1977).
- [25] Y.K. Gambhir, P. Ring and A. Thimet, *Ann. Phys. (N.Y.)* **198**, 132 (1990).
- [26] P. Ring, *Prog. Part. Phys.* **37**, 193 (1996).
- [27] R. J. Furnstahl, B. D. Serot, and H. B. Tang, *Nucl. Phys.* **A598**, 539 (1996).
- [28] R. J. Furnstahl, B. D. Serot, and H. B. Tang, *Nucl. Phys.* **A615**, 441 (1997).
- [29] H. Müller and B. D. Serot, *Nucl. Phys.* **A606**, 508 (1996).
- [30] H. Georgi and A. Manohar, *Nucl. Phys.* **B234**, 189 (1984).
- [31] H. Georgi, *Phys. Lett.* **B298**, 187 (1993).
- [32] J. J. Ruskak and R. J. Furnstahl, *Nucl. Phys.* **A627**, 495 (1997).
- [33] R. J. Furnstahl and B. D. Serot, *Nucl. Phys.* **A671**, 447 (2000).
- [34] B. D. Serot, *Lect. Notes Phys.* **641**, 31 (2004).
- [35] N. K. Glendenning, *Astrophys. J.* **293**, 470 (1985).
- [36] I. Bednarek and R. Manka *Int. Mod. Phys. D* **10**, 607 (2001).
- [37] J. Schaffner-Bielich and A. Gal, *Phys. Rev. C* **62**, 034311 (1999).
- [38] A. Chodos, R.L. Jaffe, K. Johnson, C.B. Thorne and V.F. Weisskopf *Phys. Rev. D* **9**, 3471 (1974).
- [39] B. Freedman and L. McLerran, *Phys. Rev. D* **17**, 1109 (1978).
- [40] E. Farhi and R.L. Jaffe, *Phys. Rev. D* **30**, 2379 (1984).
- [41] J. I. Kapusta, *Finite Temperature Field Theory* (Cambridge University Press)
- [42] R. C. Tolman, *Phys. Rev.* **55**, 364 (1939); J. R. Oppenheimer and G. M. Volkoff, *Phys. Rev.* **55**, 374 (1939).
- [43] M. Del Estahl, M. Centelles, X. Viñas and S.K. Patra *Phys. Rev. C* **63**, 024314 (2001).
- [44] M. Prakash, I. Bombaci, M. Prakash, P. J. Ellis, J. M. Lattimer and R. Knorren, *Phys. Rep.* **280**, 1 (1997).
- [45] G. Baym, C. Pethick, and P. Suherland, *Astrophys. J.* **170**, 299 (1971).
- [46] J. Cottam, F. Paerels and M. Mendez, *Nature* **420**, 51 (2002).
- [47] D. Sanwal, G. G. Pavlov, V. E. Zavlin and M. A. Teter, *Astrophys. J.* **574**, L61 (2002).
- [48] G. F. Bignami, P. A. Caraveo, A. De Luca, and S. Mereghetti, *Nature (London)* **423**, 725 (2003).
- [49] R. X. Xu, H. G. Wang, and G. J. Qiao, *Chin. Phys. Lett.* **20**, 314 (2003).

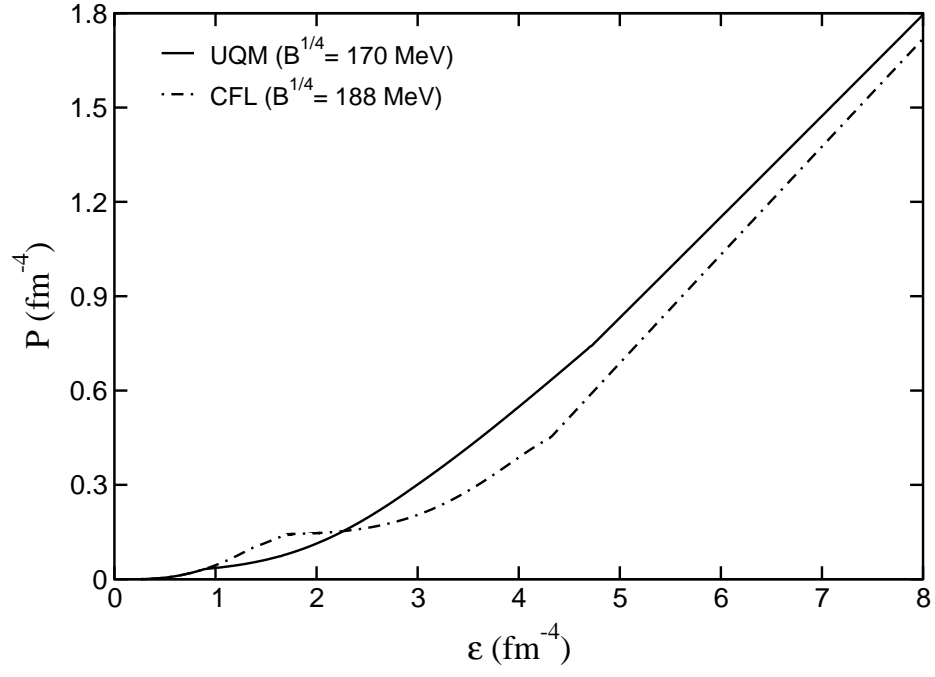


FIG. 1: Equation of state obtained with E-RMF model plus UQM (solid line) and plus CFL (dash-dotted line).

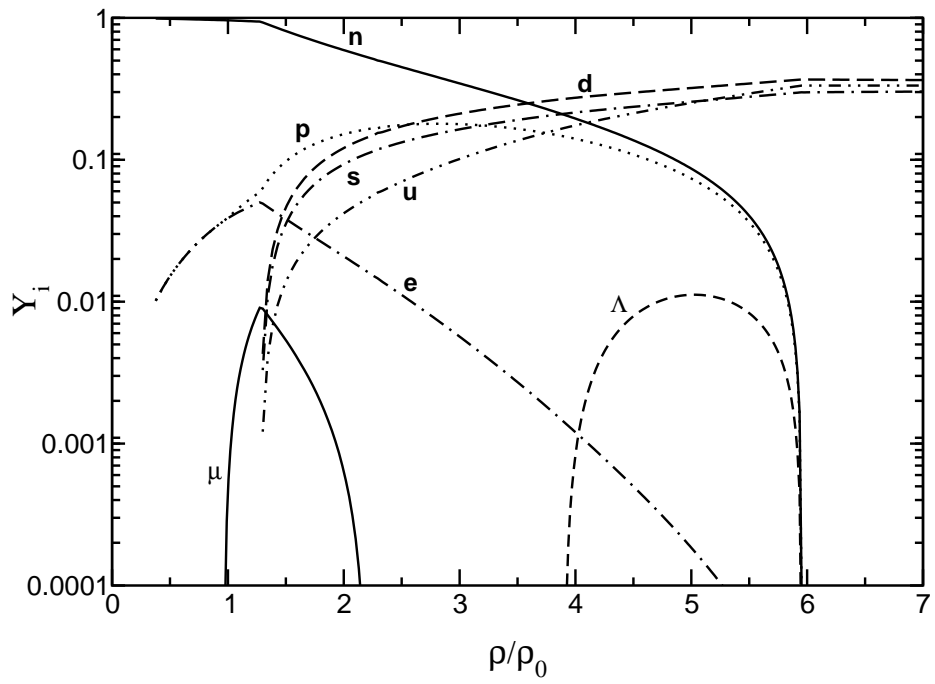


FIG. 2: Particle fractions, $Y_i = \rho_i / \rho$ for i = baryons, leptons and quarks, obtained with E-RMF+UQM ($B^{\frac{1}{4}} = 170 \text{ MeV}$).

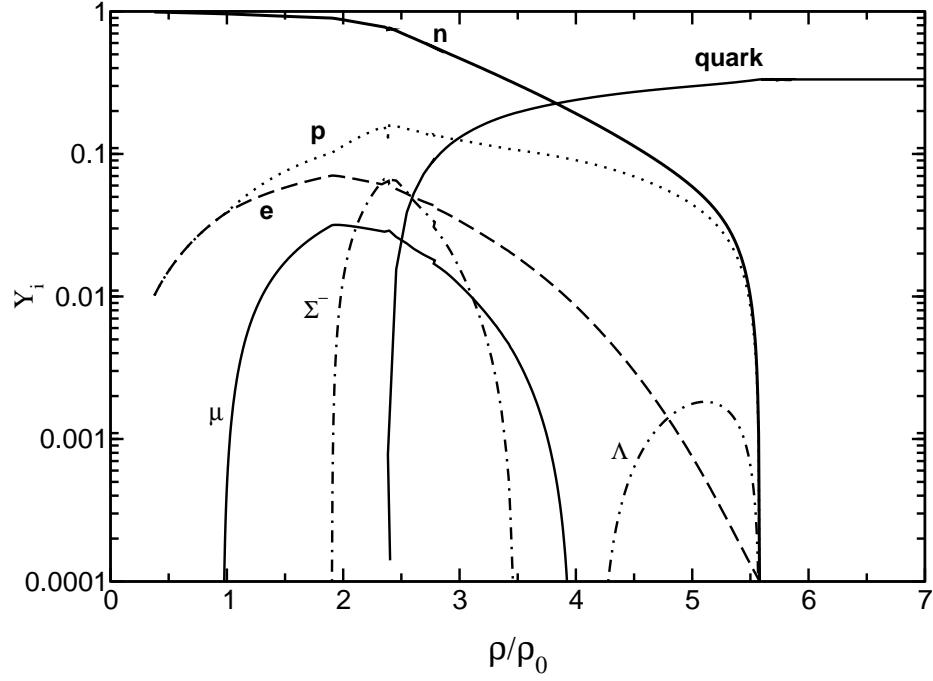


FIG. 3: Particle fractions, $Y_i = \rho/\rho_i$ for $i =$ baryons, leptons and quarks, obtained with E-RMF+CFL ($B^{\frac{1}{3}} = 188 \text{ MeV}$).

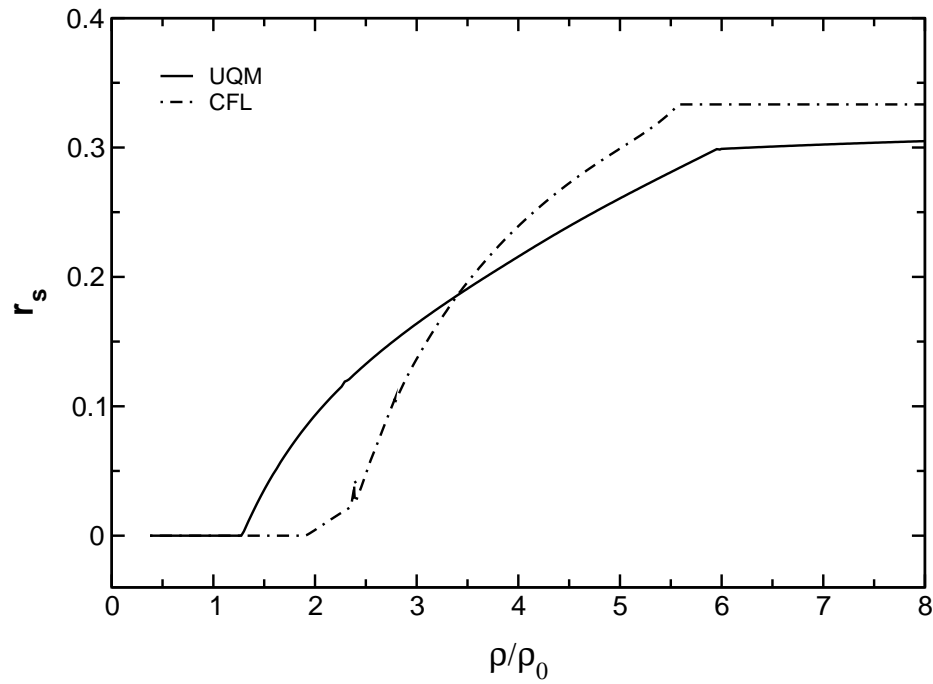


FIG. 4: Strangeness content obtained with E-RMF plus UQM (solid line), E-RMF plus CFL (dash-dotted line).

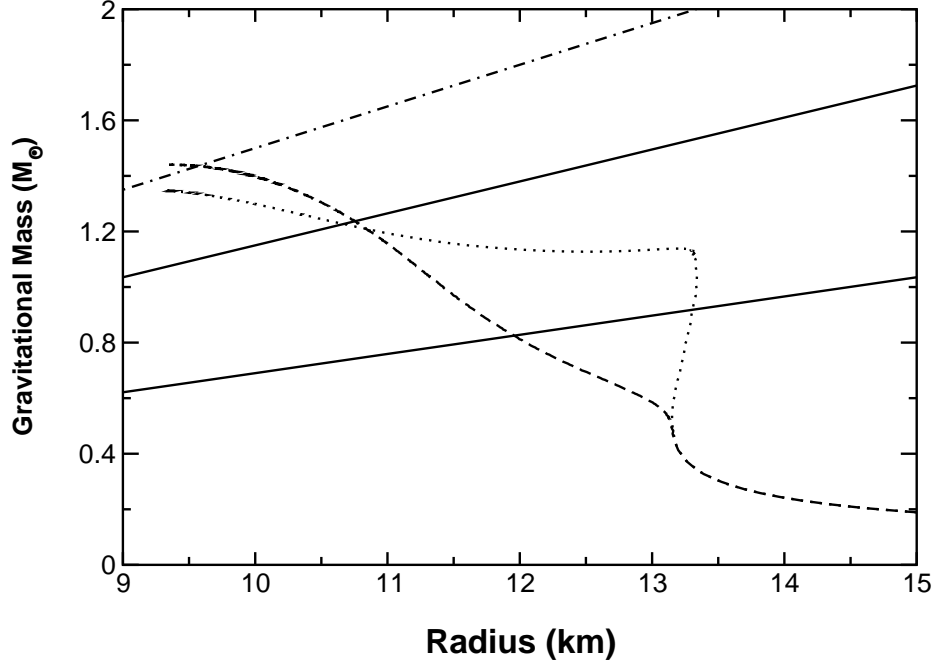


FIG. 5: Neutron star mass versus radius with E-RMF plus UQM (dashed line), E-RMF plus CFL (dotted line) with experimental observations (solid and dash-dotted lines).

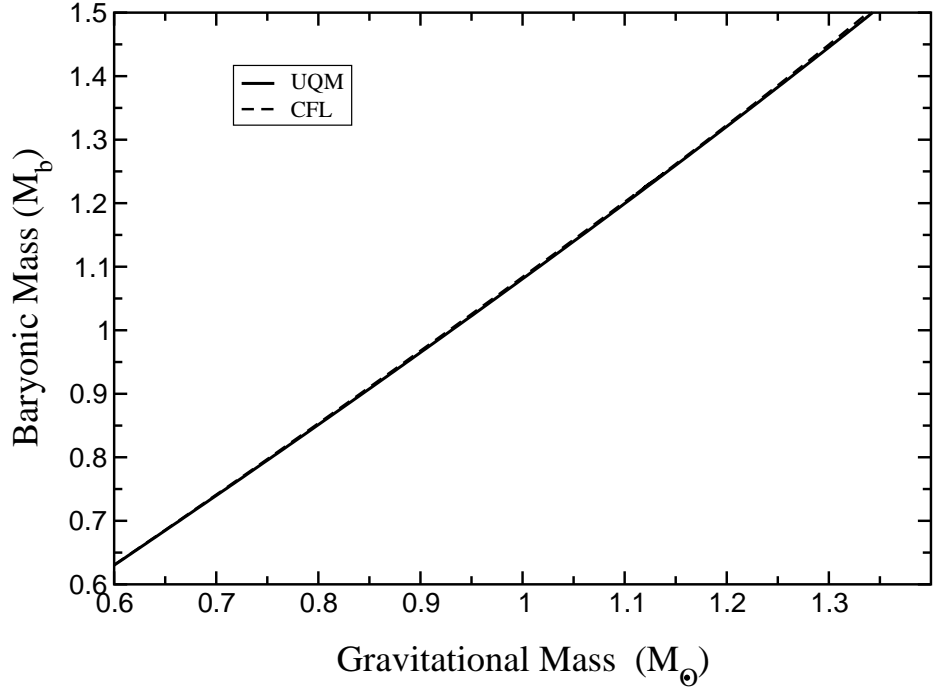


FIG. 6: Baryonic mass as a function of maximum mass of the neutron star with E-RMF plus UQM (solid line), E-RMF plus CFL (dashed line).

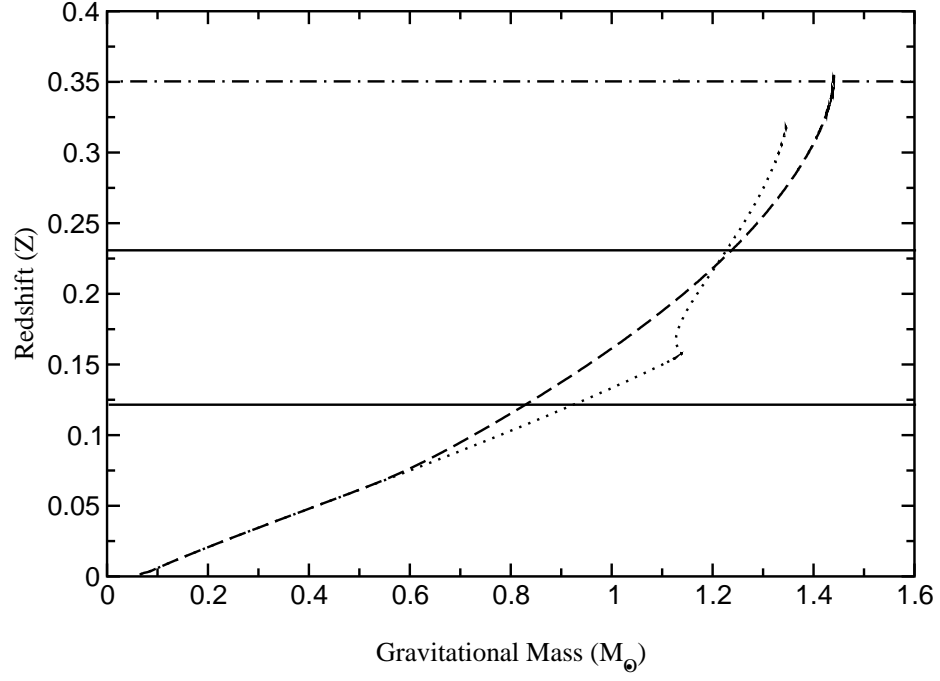


FIG. 7: Gravitational Redshift (Z) as a function of maximum mass of the neutron star with E-RMF plus UQM (dashed line), E-RMF plus CFL (dotted line) with experimental observations (solid and dash-dotted lines).